

26th International Conference on Alpine Meteorology

11 to 15 September 2000, Innsbruck, Austria



Österreichische Beiträge
zu Meteorologie und Geophysik

ISSN 1016-6254

Heft Nr. 23 / Publ.Nr. 392



CENTRAL INSTITUTE FOR METEOROLOGY
AND GEODYNAMICS, Vienna, Austria



SURFACE MEASUREMENTS DURING MAP-SOP: ENERGY AND RADIATION FLUXES IN RONDISSONE (LAGO MAGGIORE TARGET AREA)

M. Nardino, F. Calzolari, T. Georgiadis and V. Levizzani
CNR-ISAO Via Gobetti 101, 40129 Bologna, Italy

ABSTRACT

During MAP-SOP surface incoming and outgoing shortwave and longwave radiation components were measured in Rondissone, north of Turin. The momentum flux, turbulent kinetic energy, sensible heat, and subsurface heat flux were also computed from sonic anemometer continuous measurements. A first processing of the whole data set has been done and the main aerodynamic parameters computed. The surface energy and radiation fluxes were associated to the meteorological conditions for the characterisation of the turbulent pattern of the site. The spectral analysis serves the purpose of identifying the synoptic forcing on the atmospheric surface layer.

1. INTRODUCTION

One of the main objectives of the Mesoscale Alpine Programme (MAP) is a thorough investigation of the orographically-influenced precipitation events, including frontal precipitation and deep convection, and their coupling with runoff processes and prediction of flooding episodes. The project is focused on 1) the improvement of numerical predictions of moist processes over and in the vicinity of

complex topography, 2) the creation of data sets for the validation and improvement of high-resolution numerical weather prediction, and 3) the creation and test of hydrological and coupled models in mountainous terrain.

The Lago Maggiore target area was selected as the MAP target area where to tackle the scientific questions of the programme related to heavy precipitation on the southern slopes of the Alps and their relations to the complex orography of the Alpine chain. This area included the whole north-western Po Valley of Northern Italy from Turin to Milan and from the Apennine chain in the south to the Canton Ticino in the north.

The instrumentation described in the present study was used for an investigation of the planetary boundary layer (PBL) structure prior and during the Intense Observation Periods (IOP). Radiometric and turbulence measurements were continuously recorded and enter the computation of the surface radiation budget and the surface energy fluxes.

The net radiation available at the surface is given by:

$$R_n = Sw_{in} - Sw_{out} + LW_{in} - LW_{out} \quad (1)$$

where Sw_{in} and Sw_{out} are the incoming and outgoing shortwave radiation components and Lw_{in} and Lw_{out} are the incoming and outgoing longwave components.

The net radiation, obtained from radiometric measurements, is then distributed into the turbulent fluxes and the subsurface heat flux linked together by the equation of the surface energy balance:

$$R_n = H_0 + LE + G \quad (2)$$

where H_0 is the sensible heat flux, LE the latent heat flux and G the subsurface heat flux.

The turbulence measurements, obtained with a sonic anemometer, determine the value of the surface roughness length following the methodology by Sozzi et al. (1998). An alternative way to obtain the same value considers the vertical profile of the wind speed in adiabatic conditions (Stull, 1988):

$$u = \frac{u_*}{k} \ln \frac{z}{z_0} \quad (3)$$

where u is the wind speed, u^* the friction velocity, z the measurement height, k the von Karman constant (0.4), and z_0 the surface roughness length. Inverting for z_0 :

$$z_0 = z e^{-uk/u_*} \quad (4)$$

A first data analysis is presented also with the intention to understand the problems that afflicted the determination of the surface radiative and turbulent fluxes during the IOPs. Finally, the surface roughness length was computed in order to characterise the surface typology of the site.

2. MATERIAL AND METHOD

The campaign was carried out during the autumn of 1999 in the framework of the MAP experiment, starting on 8 September and ending on 5 November. The instrumentation was installed at Rondissone (45.24°N, 7.97°E, 100 m a.s.l.). The anemological and radiometric station was equipped with: a sonic anemometer (USA-1, Metek), a radiometer (CNR1, Kipp and Zonen), three thermocouples and a flux plate.

The net radiometer is used for the analysis of the radiation balance of solar and far infrared components for quantifying the net (total) radiation at the Earth surface. The solar and far infrared radiation components were measured separately.

Three thermocouples were deployed for the measurements of the skin temperature and ground temperatures at 10 and 20 cm depth; the flux plate, used for the determination of the subsurface heat flux, was buried into the ground at 5 cm depth.

The radiometric and soil heat flux measurements were recorded by a Campbell CR10 ET data-logger every minute, averaged every 10 minutes, and then stored in a Campbell SM192 memory module.

Turbulence and heat fluxes were measured through a sonic anemometer; the instrument was aligned northward with a precision of 15 degrees at a height of 3.5 m above ground. On the same mast, at a height of 1.5 m, was located the radiometer.

The data acquisition of turbulence measurements was done via a Meteoflux computer system (Servizi e Territorio, Milan) performing

real-time measurements of the three wind components and the temperature at 10 Hz. All turbulence parameters can be derived together with the sensible heat and momentum flux by postprocessing

the data with a Fortran program following the methodology by Sozzi and Favaron (1996).

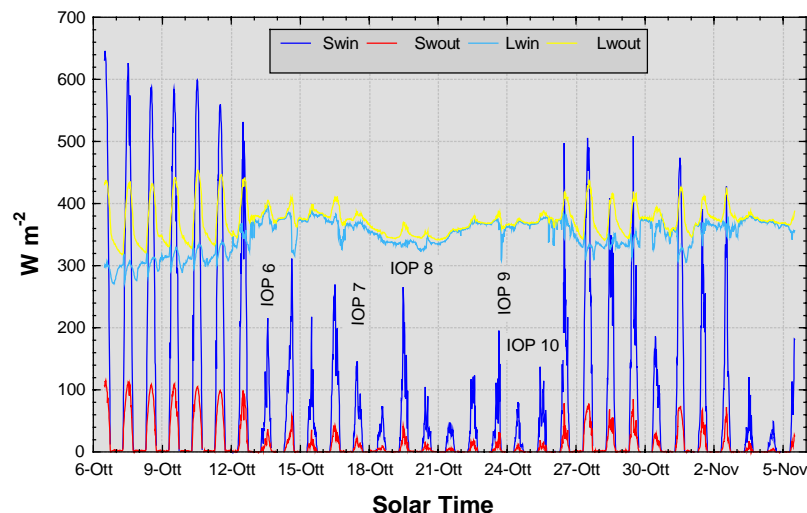


Figure 1: Time series of radiative flux components.

3. RESULTS AND DISCUSSION

3.1 Surface radiation and energy fluxes

In Figure 1 the radiative flux components obtained through the radiometric measurements are reported. The graph refers to the period between 6 October and 5 November, representative of what happened during the campaign, the IOPs in particular.

In fact, note that the shortwave radiation decreased from a maximum of about 600 W m^{-2} to a minimum of about 50 W m^{-2} during the IOPs 6, 7, 8, 9 and 10 (13-25 October). This means that a strong perturbation influenced the energy available from the sun that is

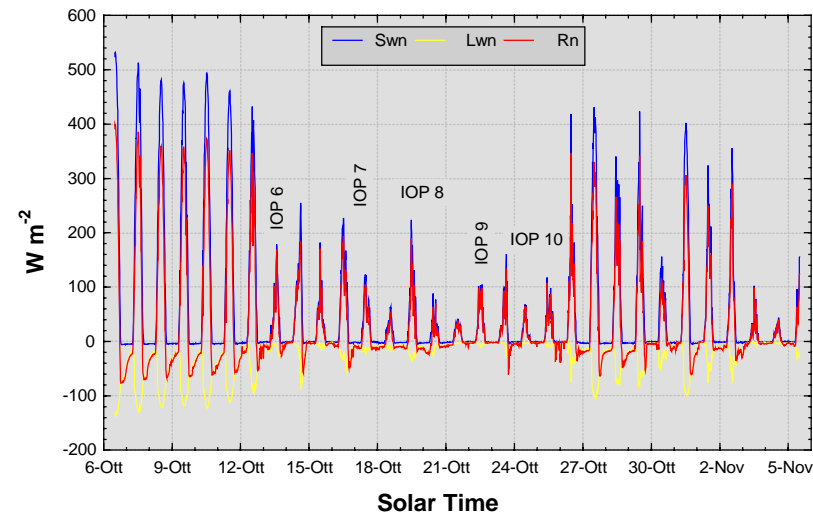


Figure 2: Time series of surface radiative budget.

substantially cut during cloudy conditions. Also the longwave values vary at the same time. Figure 2 shows the surface radiative budget. During the IOPs the net long-wave radiation is close to zero and this is due to a lower variability in the difference between the Lw_{in} and Lw_{out} with respect to the other days as evident from Figure 1.

The energy fluxes have been computed from the turbulence measurements through the eddy-covariance technique (Stull, 1988). In Figures 3a and b the turbulent kinetic energy (TKE) and the momentum flux for the same period of the radiation measurements are displayed.

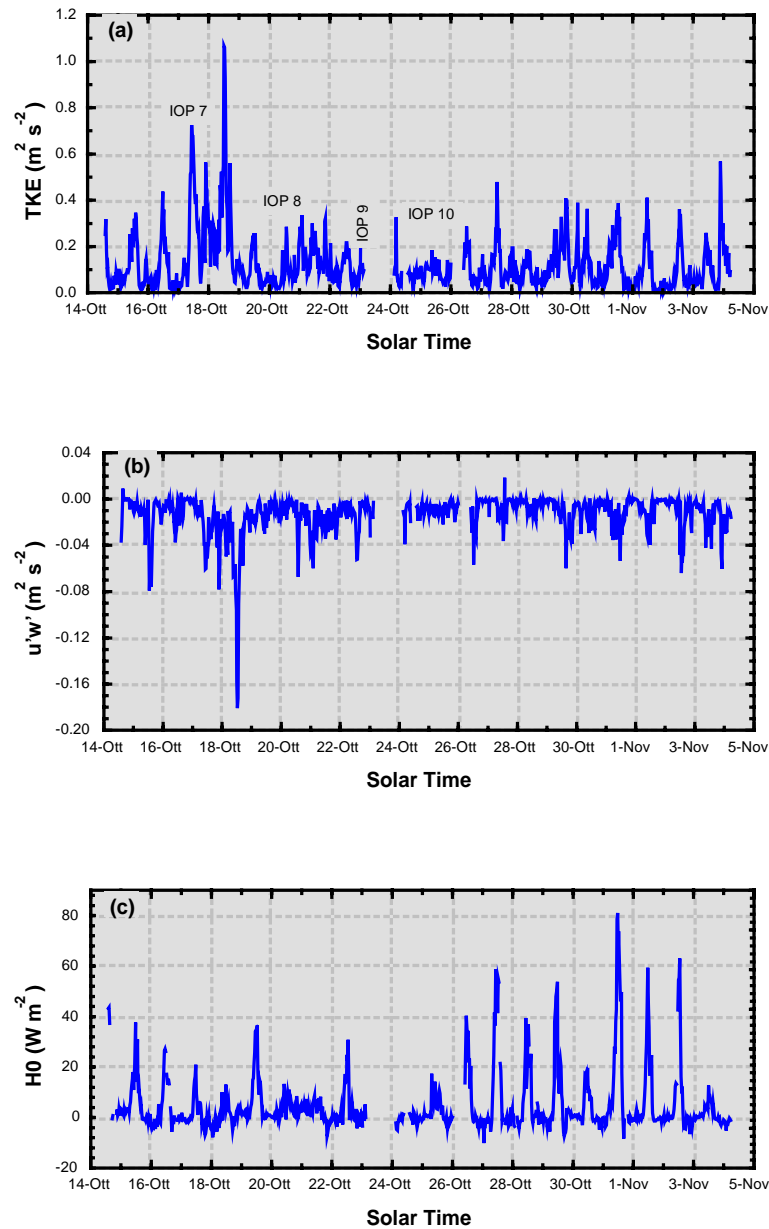


Figure 3: Time series of (a) turbulent kinetic energy, (b) momentum flux and (c) sensible heat flux.

Note that during IOP 8 (20-22 October) there was a strong increment of both fluxes while the sensible heat flux (Figure 3c) is smaller with respect to the last days of the measurement campaign. The turbulent kinetic energy, which represents the turbulence intensity, and the momentum fluxes are anti-correlated, that is when turbulence is high there is an increase of momentum flux toward the surface. The momentum and sensible heat fluxes are terms of the TKE budget equation and in our case an increase of turbulence determines higher amounts of momentum flux transferred to the surface and a decrease of released or absorbed sensible heat flux (depending on atmospheric conditions). This could be due to a small variation in the temperature gradient between the air and the surface caused by the convection generated by the perturbation.

3.2 Surface energy balance

The surface radiation balance has been computed from equation (2). Since the latent heat flux was not measured it has been determined as residual of this equation.

In Figure 4 the daily mean values of net radiation, subsurface, sensible and latent heat fluxes are shown. The greatest part of the available energy is partitioned to the latent heat flux. This means that there is a strong evaporation from the surface to the air (positive sign). The contribute of the subsurface heat flux is lower while the sensible heat flux is a third of the net radiation.

Note that during the IOPs the net radiation and the sensible heat flux drop down to a value of about 20 W m^{-2} and $5\text{-}10 \text{ W m}^{-2}$, respectively. This is due to a lower amount of shortwave radiation during the perturbation and a smaller temperature gradient between the surface and the air.

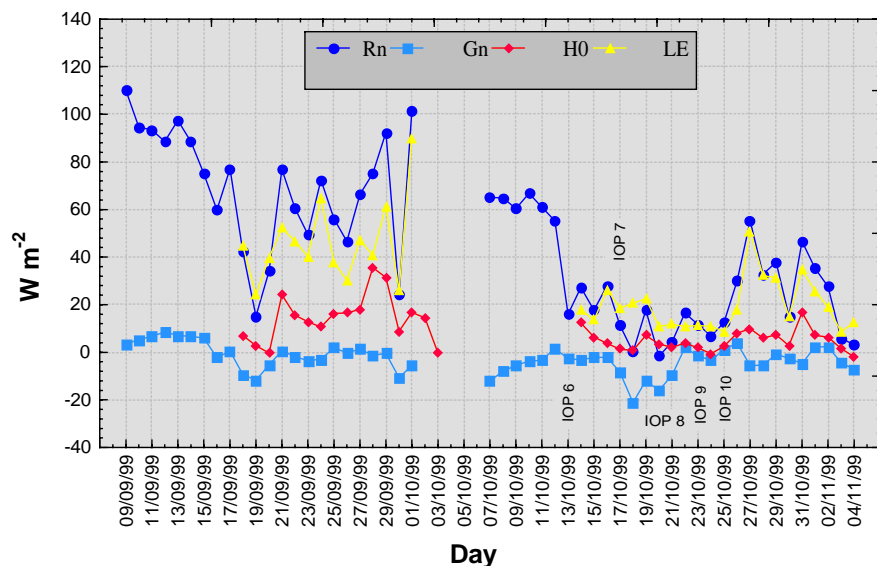


Figure 4: Daily mean energy balance terms.

3.3 The surface roughness length

The value of the surface roughness length was computed from the turbulence measurements and the polar plot is shown in Figure 5.

The mean and median values of z_0 for each wind sector were computed following the methodology by Sozzi et al. (1998) to characterise the surface around the measurement site: the median values are lower than the corresponding mean values, and are closer

to the characteristic values for grass surfaces. For this reason they can be considered as a suitable statistics that applies to the data.

The very high values obtained within the wind direction sectors between 90° and 150° could be due to ploughed land along these directions as we point out later.

For the other directions the values are typical of surface covered by non uniform grass.

The friction velocity, which can be treated as the effect of the stress winds at the ground, varies according to the surface roughness parameters and follows the behaviour of the wind speed. The scatter plot of the two velocities in Figure 6 indicates that they are linearly correlated, but there is a clear evidence of two lines depending on the wind direction. So, the data were divided considering the “data above” and the “data under” the line plotted in the graph.

Consequently, in order to obtain a mean value of the surface roughness length during the whole campaign the vertical profile of the wind speed during adiabatic condition was considered (equation (3)). The values of z_0 has been computed for both wind direction sectors as reported in Figure 7.

The very much high value for the wind sector $0^\circ\text{-}100^\circ$ ($z_0 = 0.39 \text{ m}$) is again probably due to the presence of ploughed land in that direction.

For the wind sector between 300° and 360° a typical value characterising the surface was considered ($z_0 = 0.043 \text{ m}$).

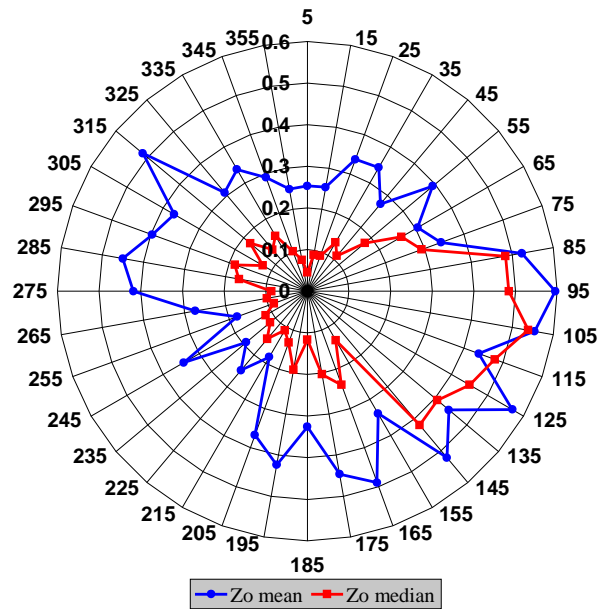


Figure 5: Polar plot of the mean and median values of the surface roughness length in meters.

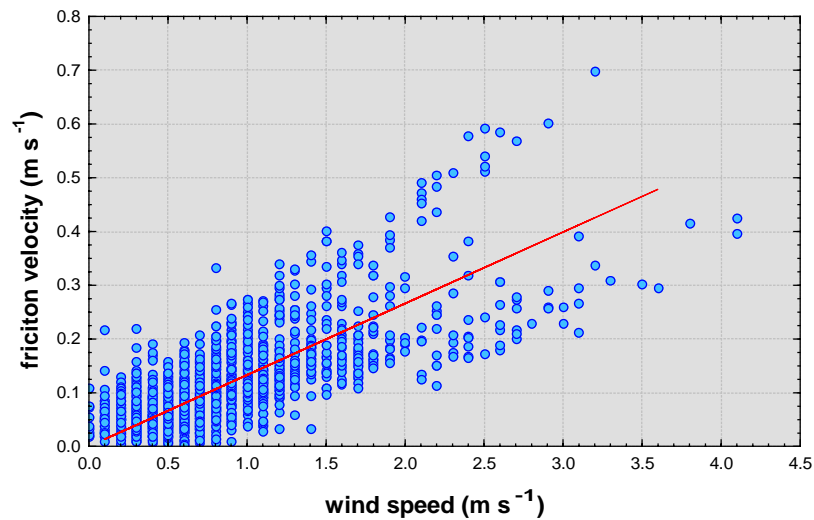


Figure 6: Scatter plot between the friction velocity and the wind speed.

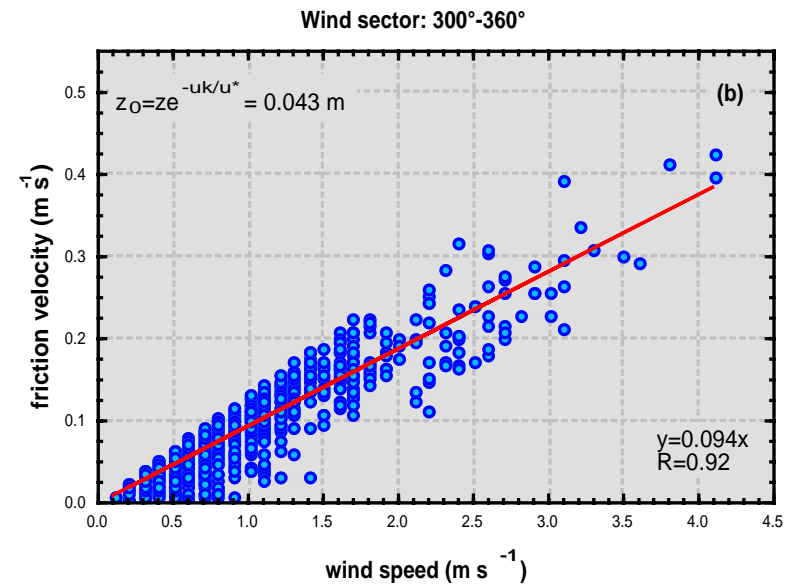
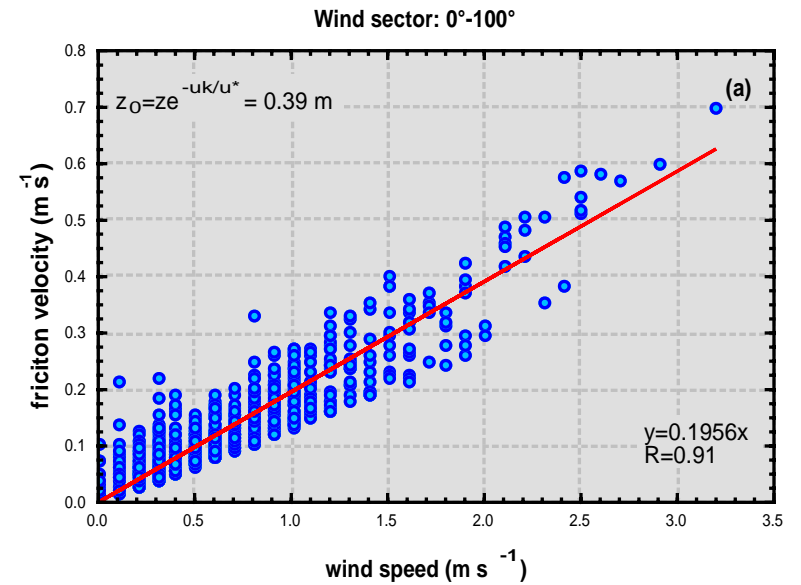


Figure 7: Scatter plot of the friction velocity versus the wind speed for (a) 0°-100° wind sector and (b) 300°-360°. Regression lines are also displayed.

4. CONCLUSIONS

The measurements show the effects of the perturbations recorded during the IOPs on the surface radiative and energy fluxes. During such events the shortwave radiation is the most influenced while the turbulence fluxes are higher except the sensible heat flux which decreases.

The two methods used for the computation of the surface roughness length are in very good agreement: in both case the value of z_0 for the wind sector 0° - 100° is higher than the values reported in the literature for that surface. This result is explained by the presence of ploughed land along this direction, which perturbed the surface measurements.

The values of the surface roughness length are acceptable for surface covered by grass.

Further investigations are necessary for the study of the turbulence spectra for the computation of the energy transported by the vortexes and the gravity waves.

Acknowledgements

Campaign and data processing were funded by Consiglio Nazionale delle Ricerche (CNR), Contract under *Progetto Strategico MAP-SOP*, and Agenzia Spaziale Italiana (ASI), Contract *Sinergia GERB-SEVIRI nello Studio del Bilancio Radiativo a Scala Regionale e Locale*.

References

- Sozzi, R., and M. Favaron, 1996: Sonic anemometry and thermometry: theoretical basis and data-processing software. *Environmental Software*, **11**, 259-270.
- Sozzi, R., M. Favaron, and T. Georgiadis, 1998: Method for estimation of surface roughness length and similarity function of the wind speed vertical profile. *J. Appl. Meteor.*, **37**, 461-469.
- Stull, R. B. 1988: *An introduction to boundary layer meteorology*. Kluwer Academic Publ., 666 p.